Sensors & Actuators: A. Physical 372 (2024) 115346

Contents lists available at ScienceDirect

Sensors and Actuators: A. Physical

journal homepage: www.journals.elsevier.com/sensors-and-actuators-a-physical

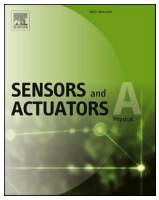

Cold and ultra-cold chain integrity monitoring via embedded resonant sensor indicators

Yee Jher Chan, Nareen Anwar, Nigel Forest Reuel *

Department of Chemical and Biological Engineering – Iowa State University, United States

ARTICLE INFO

Keywords:
Time-temperature indicator
LC resonant sensor
Ultra-cold chain irreversible temperature sensor
Wireless temperature sensor

ABSTRACT

An increasing number of products require transport at cold and ultra-cold temperatures, < 5 and −60°C respectively. Time-temperature indicators (TTIs) are used to monitor the integrity of the cold chain, however, they are frequently based on colorimetric changes that can be inaccurate for quantification and not possible to read through closed shipment materials. Here, TTIs were prototyped using microfluidic channels containing fluids (oils) that are tuned to melt above target temperatures. By coupling these TTIs to resonant sensors, the time-temperature information can be transmitted wirelessly and quantitatively by observing shifts in resonant frequency. Multiplexed TTIs containing fluids that melt at 9, 13.5, and 19.5°C are demonstrated. When coupled to the resonant sensor, the fluid flows as the temperature increases incrementally and generates a frequency shift of 3.5, 4.5, and 6 MHz at each threshold. TTI for ultra-cold environments were also designed using microfluidic channels with melt responsive fluids (ethanol). The resonant sensor coupled TTI was placed in a Styrofoam container containing dry ice, and over 1 MHz frequency shift is observed when read external to the container as the dry ice evaporates and the temperature exceeds −35°C. This augurs potential uses in inexpensive monitoring of food and pharmaceutical shipments that must remain cold for adequate quality.

1. Introduction

Cold chain logistics involves the storage, transport, and distribution of temperature sensitive products with minimal product loss. However, significant temperature aberrations during the transportation and distribution have been observed that could compromise the product quality [1,2]. Literature reviews in the cold chain logistics have been performed and demonstrated that the importance of temperature monitoring as a prominent quality control measure [3–5]. Although other parameters such as humidity could have an impact on the product degradation [6], temperature remains as the most prominent indicator of the product quality. While some products such as dairy goods and drugs can be stored at refrigerated temperature (2–8°C), increasing number of products has required an ultra-cold environment (<-60°C) to preserve their functionality such as many recent mRNA vaccines and biomolecules. For products requiring refrigerated temperatures, they can be enclosed in a temperature insulating container with ice (often used for small quantity) or they can be transported with a continuous cooling source. For products at ultra-cold environment, the products are transported in Styrofoam box with dry ice or in dewars with liquid nitrogen.

Currently, the widely used method of monitoring the temperature profile is through the radio frequency identification (RFID) technology integrated with an electrical-based temperature sensor [7,8]. The types of electrical-based temperature sensor are thermistor, thermocouple, and resistance temperature detector. Each of these has different cost and accuracy and can be selected according to the application. The RFID reader interrogates the tags that are attached onto the packages and obtain the temperature measurements. By incorporating the Wireless Sensor Networks, the product location and the temperature profile can be traced remotely in real time [9,10]. However, this modality typically requires a power source and microchip for every sensor which results in higher cost and reduced ability to scale up when the products are broadly distributed. In addition, it is commonplace that the temperature information is not transmitted during the transportation, i.e. scanned at terminal points [11].

Alternative to the electrical-based temperature sensor are temperature indicators that have an irreversible response towards temperature. Vivaldi et al. utilized copper doped ionic liquid to generate an irreversible change in impedance of an RFID tag when temperatures exceeded the 8°C threshold [12]. Another approach used two RFID tags

* Corresponding author.
E-mail address: reuel@iastate.edu (N.F. Reuel).

https://doi.org/10.1016/j.sna.2024.115346
Received 22 August 2023; Received in revised form 22 December 2023; Accepted 4 April 2024
Available online 6 April 2024

with an embedded metal plate in ice interfering with one of the tags [13,14]. When the temperature rises, the ice melts, and the metal plate shifts towards the tag to reduce backscattering signal of one tag while improving signal of the other. Lorite et al. incorporated a microfluidic critical temperature indicator with an RFID tag that responds at the critical temperature around 18–19°C [15]. Although these approaches provide an adequate indication, these approaches rely on the change in backscattering power, which limits tunability of the sensor. Chipless RFID sensor is another simpler approach that can be applied in this application [16–18]. Due to the inherent sensitivity towards the environment, the resonant frequency can be used to track the parameter of interest (e.g. temperature) when integrated with a responsive material [19].

Although temperature indicators can inform when a temperature threshold has been exceeded, the product's shelf life can still vary greatly at elevated temperatures. Time-temperature indicators (TTI) that inform both the temperature and the amount of time where the temperature has exceeded are of greater interest [20]. TTIs can be classified into diffusion-based [21–23] and reaction-based indicators [24–26]. For instance, a reaction-based indicator was developed by Sun et al. based on the reaction between amylase and starch [27]. The hydrolysis of starch catalyzed by amylase creates a colorimetric change in the presence of iodine and that response is both time and temperature dependent. Choi et al. developed a TTI mat using thermoplastic polyurethane nanofiber [28]. The mat is opaque at −20°C and 2°C and becomes transparent over 0.5–22.5 hr depending on the polymer composition and film thickness when warming up to room temperature. For diffusion-based indicators, temperature-responsive fluids are used to measure the extent of temperature aberration. Jafry et al. designed a fan-shaped nitrocellulose membrane and tested with the flow of oleic, octanoic, and decanoic acid through the capillary action [29]. Other diffusion-based TTIs that are commercially available are 3 M™ Monitor Mark™ and WarmMark®.

Most of the TTIs rely on color changing indicators that must be observed by eye [23,30–33], which limits their applicability in the many opaque containers and packaging used in cold chain logistics, such as a large pallet of meat shipped internationally. Inductive-capacitive (LC) resonant sensors offer a niche solution in this application by enabling a wireless interrogation modality to the TTIs. LC sensors are chipless sensors that have an inherent resonant frequency in the radio frequency regime [34]. The resonant frequency is dependent on the permittivity around the sensor and their ability for sensing in a closed system has been demonstrated. For instance, the resonant sensor can be embedded in bandages [35] and garments [36] to monitor the wound, skin, and sweat properties through the changes in resonant frequency. In addition, LC sensors are chipless and are readily scalable (roll to roll manufacturing, no integrated circuit placement), which is cost effective when comes down to wide distribution in cold chain logistics [37]. Integrating the LC sensors to detect the permittivity changes of TTIs could therefore be valuable in monitoring the integrity of cold chain logistics.

In this work, LC sensors are coupled to a TTI to demonstrate the utility in the cold chain and ultra-cold chain applications. A TTI is first designed based on the fluid flow within a microfluidic channel. Temperature-responsive fluids are screened for the target range of 2–8°C. Mixtures of fluids are also screened for tuning the temperature thresholds up to 21°C. A resonant sensor is then coupled with the TTI to test for the wireless transmission of the temperature cue. Finally, another TTI integrated resonant sensor is designed to work in the ultra-cold environment.

2. Methods

2.1. Microfluidic channel fabrication

The TTI designs were created in Inkscape with different trace colors indicating different cut settings. Different designs were used for different experiments as described below. Glowforge laser cutter was then used to pattern a 2 mm thick acrylic sheet. The thorough cut was achieved using full power setting and a speed of 150 whereas the partial cut was achieved using full power setting and a speed of 500. This created a cross-sectional channel with a depth of 840 μm and a width of about 500 μm (see Section 1 of Supporting Information). After laser cutting, the surface facing the laser was covered with a packaging tape to enclose the channel. On the other surface, the reservoirs were partially or fully covered (detailed in each section below) to hold the fluid.

2.2. Working fluid identification

The prototype for testing the melting of fluid is illustrated in Fig. 1 and Section 1 of Supporting Information. After patterning the channels using laser cutter, packaging tape (3 M Scotch heavy duty) was used to seal the channels and partially cover the reservoirs. Peanut oil (LouAna) or mixture with coconut oil (Spectrum) at a volume ratio of 5:1, 5:3, and 1:1 was used to fill up the channel. The chip was then brought to freeze at −20°C for about an hour or until the liquid was frozen. The top reservoir of the chip was added with dyed solution and chilled for another 5 minutes. The chip was transferred into a portable freezer (AstroAI) that was set at −2.8°C and placed vertically. The temperature was incrementally ramped by 1.5–2.5°C about every 2 hours until the fluid flow was observed. A thermocouple (Amprobe TMD-56) was used to obtain the temperature profile of the prototype or TTIs during the experiments.

2.3. Cold chain TTI setup

The TTI design for refrigerated temperatures is modified from the design above and illustrated in Fig. 2. The schematic of the TTI setup can be found in Section 2 of Supporting Information. Briefly, 9 μL of each peanut oil, C1, and C3 oils were added into three separated channels of a TTI with a resonant sensor attached. The resonant sensor was fabricated as described previously in [37]. Briefly, a mask of the spiral resonant sensor design was printed onto a copper laminate, Pyralux®, using a solid ink printer (Xerox ColorQube). The patterned copper laminate was then immersed into the etching solution containing 1:1 vol ratio of 3 wt % hydrogen peroxide and concentrated hydrochloric acid. Finally, the mask was removed by acetone rinse. After the oils were frozen, 30 μL of dyed saline solution was added into the reservoirs through the smaller inlet circle. The TTI was brought to the portable freezer at −2.8°C. Similar to above, the temperature was increased incrementally by 1.5–2.5°C every 2 hours until the fluid flow was observed with a camera. Meanwhile, a 4 cm diameter reader coil connected to a vector network analyzer (Copper Mountain TR1300) was used to interrogate the resonant sensor while a webcam was simultaneously capturing time lapse images. For transient temperature perturbation, the temperature of the portable freezer was increased to the maximum for about 30 minutes and then returned to 2.8°C.

2.4. Ultra-cold chain TTI setup

For ultra-cold chain environment, pure ethanol was added to 15% (w/w) calcium chloride solution to create a 40% ethanol saline solution. The TTI design was modified to accommodate the fluid property and is illustrated in Fig. 5. The detail of the setup is depicted in Section 3 of Supporting Information. Briefly, 300 μL of ethanol solution was added into the reservoir and the TTI coupled with resonant sensor was frozen in a Styrofoam box with dry ice. After freezing, the TTI was attached onto the side surface of the Styrofoam box using a VHB double sided tape. A 4 cm diameter reader coil was used to interrogate the resonant sensor through the Styrofoam box (thickness = 3.8 cm). After the reader coil has been set up, some dry ice was removed to accelerate the melting process.

2.5. Sensor performance characterization

Since the sensor monitors the temperature exceedance and time of exceedance simultaneously, we defined the sensor performance using several metrics: 1) Working range: Time: the amount of time the working fluid flows through the channel. Temperature: defined by working fluid; 2) Sensitivity: The resonant frequency shift after the temperature exceeded the working fluid melting point; 3) Linearity: The correlation between resonant frequency and time exceeding the engineered threshold; 4) Noise: Maximum fluctuation of resonant frequency before the TTI is activated; 5) Resolution: Time to induce a noticeable change.

3. Results and Discussion

3.1. Microfluidic channel working principle

A microfluidic channel was utilized to transduce the temperature through the temperature-sensitive fluid within the channel. The microfluidic channel was fabricated by laser cutting an acrylic sheet, allowing a simple and cost-effective manufacturing process. A fully cut setting was used to create the reservoirs (black circle) and a partial cut setting was used to create the channels (Fig. 1a). After the microfluidic chip was fabricated (see Methods for detail), the channels were filled with temperature transducing fluid and chilled. Dyed solution was added into the reservoir for visualization purpose. With increasing temperature, the stagnate fluid was expected to vary its physical properties and flows within the channel. The driving force of this system is obtained predominantly through gravity. No observable fluid movement was obtained through capillary forces at the scale of these channel sizes. Proper orientation could be maintained on most large pallet shipments (e.g., global meat or pharmaceutical shipments). For smaller individual packages where orientation could vary, the design would need to be reconsidered to make it gravity independent.

3.2. Temperature transducing fluid

For the fluid of choice, a panel of candidates with melting point around the refrigerated temperature (2–8°C) have been investigated including dimethyl sulfoxide, glycerol, and oils. Although all the options are considerably safe and cost-effective, dimethyl sulfoxide was able to leach into the porous structure and was therefore difficult to control. Glycerol was not able to stagnate despite at lower temperatures. Commercially available edible oils including peanut oil, avocado oil, and olive oil were also tested. Although the freezing point of the different oils are similar, peanut oil took the least time to solidify and melt likely due to the inherent nucleation property resulting from its glyceride compositions. To test the melting property of peanut oil, the microfluidic channel containing peanut oil was first frozen at −20°C for about an hour. The acrylic chip was then transferred into a portable freezer (AstroAI) at around 0°C and placed vertically and the temperature was incrementally increased every hour. When the temperature was increased to above 6°C, the peanut oil melted and flowed into the bottom reservoir.

Another advantage of oil is its ability to increase the melting temperature when mixed with other glycerides with less carbon-carbon π interactions. For this purpose, coconut oil was chosen to form a mixture with peanut oil due to its higher composition of lauric acid, a saturated fatty acid. Peanut oil was mixed with coconut oil at a volume ratio of 5:1, 5:3, and 1:1, denoted as C1, C3, and C5, respectively. Similarly, after freezing the oil mixture within the channel for about an hour, the chip was transferred to the portable freezer and the temperature was ramped incrementally by 1.5–2.5°C every two hours (Section 1 in Supporting Information). A small amount of dyed water was added into the top reservoir prior to the temperature ramping to assist visualization. The mixture C1, C3, and C5 melted when the temperature exceeded the thresholds 12.5°C, 19°C, and 22°C, respectively (Fig. 1c). This suggests that the threshold temperature can be adjusted broadly by tuning the sensor fluid mixture melt point above the target temperature.

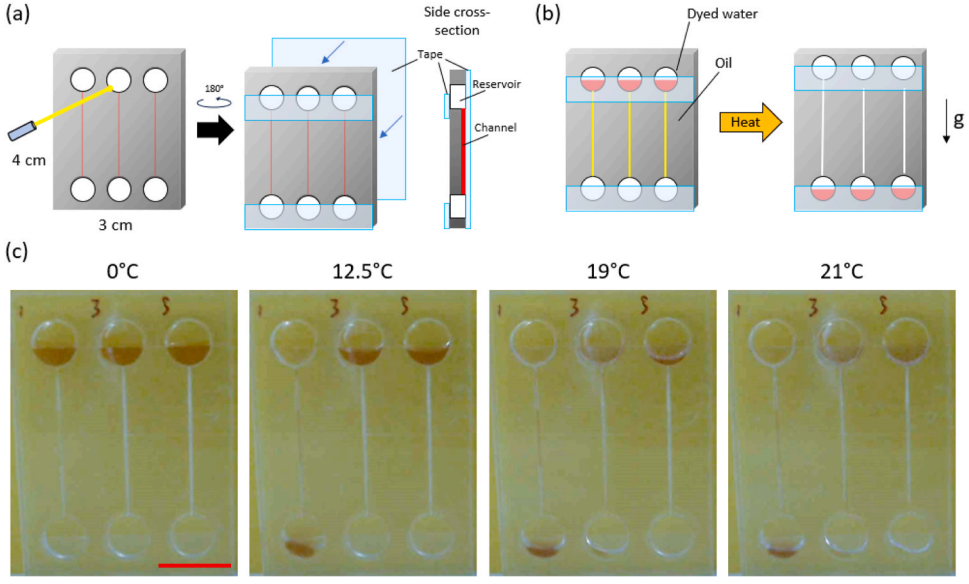

Fig. 1. (a) Schematic of microfluidic channel fabrication process. Microfluidic channel was fabricated via laser ablation of an acrylic sheet. Reservoirs were cut through (black outline) whereas channels were partially cut (red outline). Transfer tape fully covers the laser-cut side of the acrylic to fully seal the channels. The reservoirs were partially sealed on the opposite side to allow for fluid handling. A side cross-sectional view of the final design is shown. Scale bar = 1 cm. (b) Schematic of the microfluidic chip working as a temperature indicator. The channels were filled with temperature-responsive fluid and the top reservoirs are filled with dyed water to improve visualization. When temperatures exceeded the threshold of the fluid, the dyed water flowed into the bottom reservoir. (c) Melting temperature identification of the mixtures containing 5:1, 5:3, and 1:1 vol ratio of peanut oil to coconut oil.

3.3. Time-temperature indicator design

Most of the temperature indicators generate an irreversible, binary signal upon perturbation. This could result in a high chance of false positive signal due to random transient temperature spikes (e.g., a short exposure to high temperature is reported the same as long exposure). Time-temperature indicators can ideally provide the temperature history profile and thus translate the product's quality more confidently. A microfluidic channel is again suitable for this purpose by transducing the time information into the extent of fluid flow within the channel. To achieve this, a few modifications were implemented on the previous microfluidic prototype. First, the microfluidic system consists of only a single reservoir and a channel that forms a loop with the reservoir (Fig. 2a). A few inlets were also created for fluid management (see Materials and Methods and Section 2 in Supporting Information). Eventually, this creates a closed microfluidic system and eliminates the concern of leaching undesired compounds into the product. Next, the channels are partially filled with oil such that the fluid tip within the channel flows in the opposite direction of gravity. This improves the flow consistency by eliminating huge density contrast of air against the liquid within the channel. After the oil within the channel was frozen, the reservoir was filled with calcium chloride solution to improve the electrical signal as described below. A schematic of the working principle of the microfluidic system is illustrated in Fig. 2b.

3.4. LC resonant sensor integration

Most TTIs rely on colorimetric changes or require visualization, which is impractical to apply on the opaque materials that are commonly used to pack and wrap shipped products. LC resonant sensing systems have the advantage of being wirelessly interrogated (Fig. 2c). The resonant sensor has a resonant frequency which is dependent on the sensor environment's permittivity. When integrated with the TTI, the flow of fluid can change the surrounding permittivity of the resonant sensor, which can in turn be interrogated wirelessly to obtain the temperature cue (Fig. 2d).

In order to couple the TTI to the resonant sensor, a few design considerations on the microfluidic chip have been implemented. First, the oil consists mainly of non-polar compounds that do not provide an acute contrast in permittivity compared to the environment (air), resulting in a low sensitivity on the resonant sensor. To resolve this, the channel was partially filled with oil and the reservoir was filled with calcium chloride saline solution. This configuration enables the oil to serve as a switch and drive the overall flow of the fluid in the channel. Saline solution was used due to its lower melting temperature than oil and immiscibility with oil. It can also reduce evaporation rate as well as increase the sensitivity of the resonant sensor. When the oil melted within the channel, the saline solution flowed from the reservoir straight down to the bottom of the channel. This configuration maximizes the resonant sensor sensitivity by spanning through the entire sensor. The design of the microfluidic system also generates sufficient tension to hold the saline solution in the reservoir despite the chip being rotated at any angle.

The design considerations of the resonant sensor are determined based on the interrogation distance, the sensitivity, and the manufacturing cost. Generally, a larger resonant sensor has a longer interrogation distance. The resonant sensors used in this study have an outer diameter of around 4 cm. This allows for the interrogation distance to go up to about 5 cm in air and through non-metal materials, which is sufficient to be interrogated through most of the isothermal container designs. However, the interrogation distance also indicates that the resonant sensor signal is susceptible to interferences within that range. The microfluidic channel is therefore coupled directly to the resonant sensor to achieve maximum sensitivity while minimizing interference as the effect of interference decreases exponentially with the distance away from the sensor.

3.5. Multiplexed TTI integrated resonant sensor

The resonant sensor and the TTI design allows up to three microfluidic channels to be integrated into a single chip. This allows three fluids with various temperature properties to be simultaneously detected. We tested this design with pure peanut oil, C1 mix, and C3 mix that correspond to temperature thresholds at 6°C, 12.5°C, and 19°C, respectively. The resonant sensor was integrated to the TTI and was interrogated using a reader coil connected to a vector network analyzer

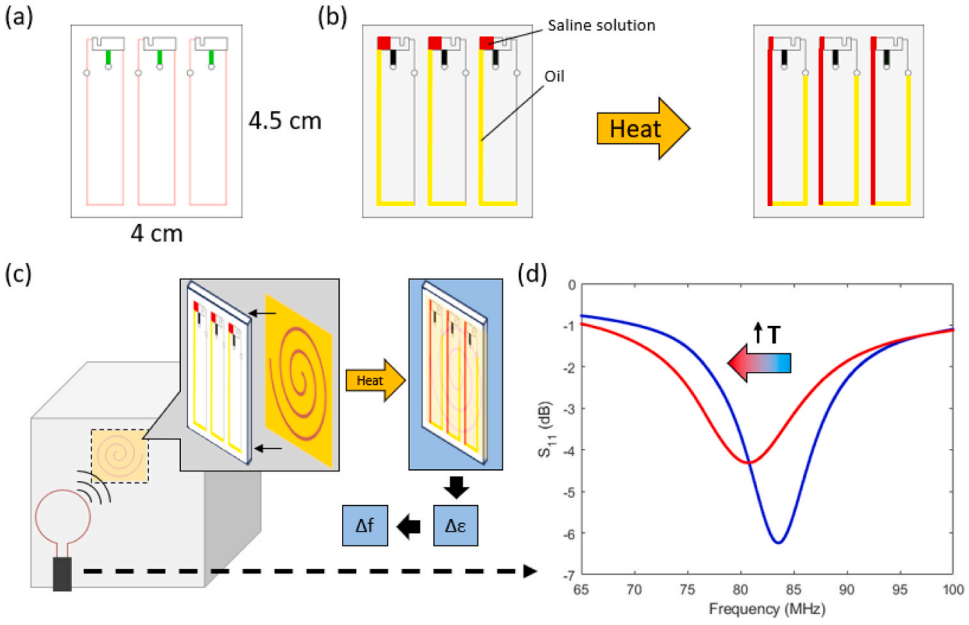

Fig. 2. (a) Enclosed microfluidic TTI design. Black outlines were cut through whereas red and green outlines were partially cut. (b) Schematic of the TTI in operation before and after exceeding the temperature threshold showing fluid movement. (c) Schematic of the operating principle of TTI integrated with resonant sensor to wirelessly assess the product quality in cold chain logistics. Flow of saline solution induced a change in permittivity around the sensor ε, which then resulted in a change in resonant frequency, f. (d) Illustration of the resonant sensor response before and after the temperature perturbation as reflected by the TTI.

for reflectance measurement. Although the mixtures began melting at those desired temperatures, we only observed noticeable flow when the temperature exceeds 9, 13.5, and 19.5°C in this TTI design. Before the temperature was increased above 4°C, the resonant frequency remained almost constant (± 0.11 MHz). When the temperature was increased to the range of 6–12°C, the saline solution flowed in the channel containing the pure peanut oil and created a 3.5 MHz shift in the resonant frequency whereas the fluid in the other two channels remained stagnant (Fig. 3). When the temperature was further increased to the range of 9.5–15.5°C, the TTI containing the C1 mixture was activated and generated an additional 4.5 MHz shift in the resonant frequency. Finally, when the temperature was set in between 13.5 and 20.5°C, the TTI containing C3 mixture started flowing and generated a 6 MHz shift in the resonant frequency. Since the TTIs are aligned with increasing temperatures thresholds, activating the TTI with higher temperature thresholds would always activate the TTIs with lower temperature thresholds. The resonant frequency fluctuated no more than 0.5 MHz when the fluid was stagnant. The total time taken for the fluid to flow across the channel were 71, 12, and 90 minutes for channels containing peanut oil, C1, and C3, respectively. Different response times were observed between the channels due to the variation of heat stress provided onto the system. When looking at the resonant frequency response only at temperatures above the thresholds, we observed that the resonant frequency started shifting after 5 minutes exceeding the temperature thresholds (Section 4 in Supporting Information). Fitting the response curve with a linear model resulted in an average slope of −0.10, −0.27, and −0.10 MHz/min for peanut oil, C1, and C3 channels, respectively. Given the noise (0.11 MHz) before the TTI was activated, we deducted that 4 minutes or 0.4 MHz to obtain a signal-to-noise ratio above 3 to confirm the exceedance of temperature.

3.6. Transient temperature perturbation response

For storage spaces involving a continuous cooling source, a breakdown in the cooling system during the transportation could not be detected using the electrical based temperature sensor when remote transmission is not available. This prototype enables an irreversible response upon the temperature perturbation incurred throughout transportation due to the irreversible fluid flow within the channel. When the cooling source is returned, the TTI should indicate if the transient temperature change has implied any significant damage on the products. This transient temperature change can also happen during the handling or transferring of the products. To exemplify this condition, the multiplexed TTI coupled resonant sensor design, as shown above, was brought to above 9°C for about 30 minutes and then returned to 2°C. The channel containing peanut oil flowed to halfway through the channel and then was refrozen while the other channels remain stagnant (Fig. 4a). The resonant frequency shifted by about 0.6 MHz throughout the temperature aberration and stayed constant when the temperature returned to below 9°C (Fig. 4b). The shift of resonant frequency was observed 13 minutes after the temperature exceeds 9°C and the stabilized signal was observed 10 minutes after the temperature returned to below 9°C. This shows that the sensor provides a fast response time and maintains its functionality after refreezing cycle.

3.7. Ultra-cold chain

An increasing number of products in the biotechnology and pharmaceutical industry require an ultra-cold environment for product integrity. Those products are typically transported with dry ice or within Dewars with liquid nitrogen. We have selected dry ice in a Styrofoam container as the model system. As the dry ice evaporates over time, the temperature within the container creates a gradient that can be used to signal the operators when actions are needed, such as placing the sample in a −80°C freezer.

Similar to the approaches described above, a microfluidic channel was designed using laser cutting (Fig. 5a). For the indicator fluid, ethanol solution was selected due to ease in adjusting the melting temperature. Calcium chloride was also added into the ethanol solution as its hygroscopic property allows it to maintain the signal for a longer time. Since the solution would remain frozen, the reservoirs were designed to be open to atmosphere. A longer channel was also used due to the greater capillary forces of the ethanol solution. A schematic of the TTI coupled resonant sensor in operation is illustrated in Fig. 5b. The TTI coupled resonant sensor was then placed inside a Styrofoam container and a reader coil interrogated the sensor through a wall thickness of 3.8 cm (Fig. 5c). As the dry ice evaporated, the temperature within the container gradually increased and the ethanol solution melted as the temperature increased beyond −35°C, resulting in about a megahertz shift in the resonant frequency over 34 minutes (Fig. 5d). The response resulted in 0.025 MHz/min when fitted using a linear model (Section 4 in Supporting Information). Considering that the resonant frequency shift was within 0.1 MHz before the TTI was activated, a total of 12 minutes of 0.3 MHz (S/N > 3) was required to justify the sensor response. Since the ultra-cold environment often creates frosts that hinder visualization-based sensors, these results showed the utility of resonant sensor to overcome the challenge by transmitting the temperature cue through a fully enclosed system. We have included a

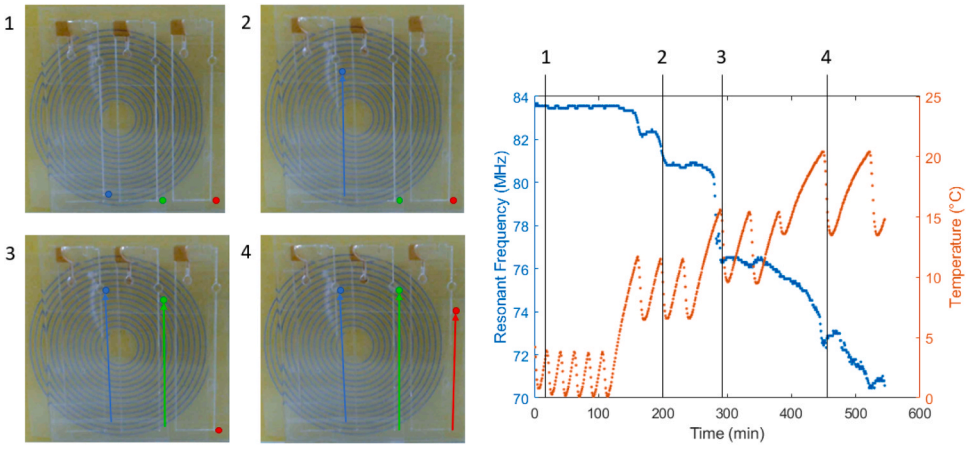

Fig. 3. (Left) Real-time images of the multiplexed TTI coupled resonant sensor at different time points as shown on the right. Colored dots beside the channels indicate the fluid level, in which blue, light green, and red colors correspond to the channels containing pure peanut oil, C1, and C3, respectively. (Right) The resonant frequency response of the sensor as the portable temperature was increased incrementally. Note our inexpensive portable cooler uses a bang-bang controller (binary on/off) to maintain temperature as evidenced by the oscillating signal.

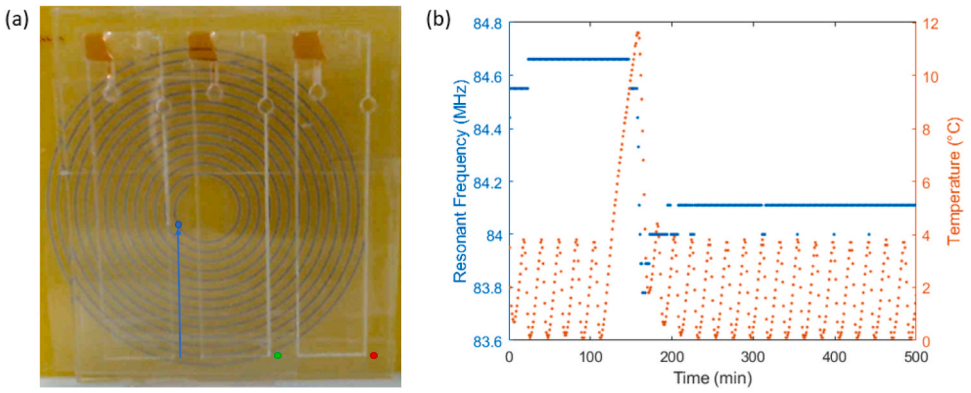

Fig. 4. (a) Real-time image of the TTI coupled resonant sensor after the transient temperature perturbation. The fluid within the channel flowed and was refrozen when the temperature returned to below 9°C. (b) Resonant frequency response towards a transient temperature perturbation to indicate irreversible response of the signal while being able to continue monitoring the product quality.

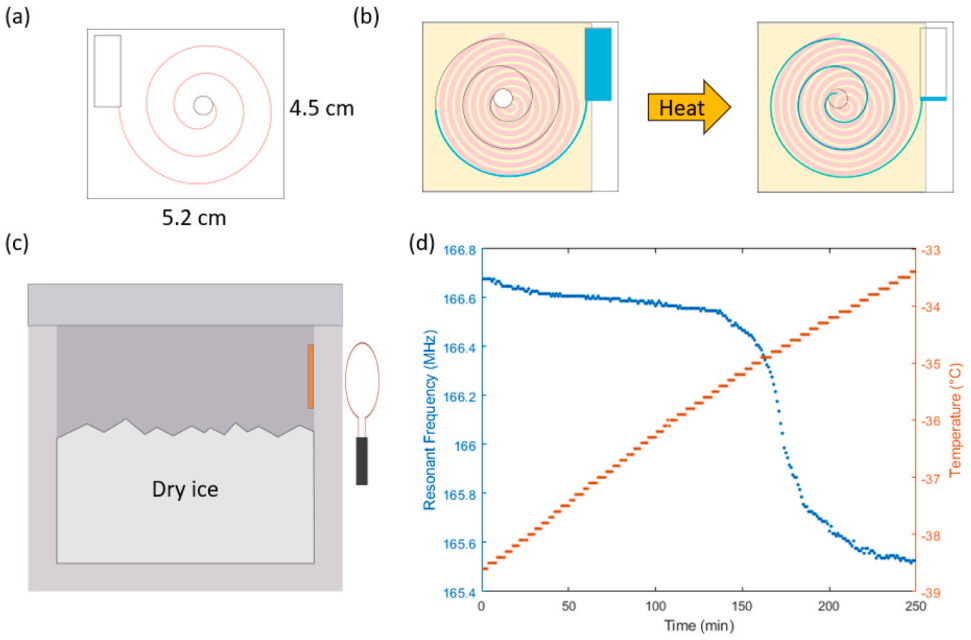

Fig. 5. (a) Microfluidic TTI design for ultra-cold temperature. Black outlines were thoroughly cut whereas red line was partially cut. (b) Schematic of the TTI in operation before and after exceeding the temperature threshold. The fluid used was 40% ethanol solution containing calcium chloride. (c) Schematic of the experiment setup. Reader coil was used to interrogate the resonant sensor through a thickness of 3.8 cm. (d) Resonant frequency response as dry ice evaporates. The ethanol solution melted at around 35°C.

comparison between different types of TTIs in Section 5 of Supporting Information.

4. Conclusion

In this work, time temperature indicators were coupled to resonant sensors to wirelessly monitor the dynamic temperature profile in cold chain applications. The TTI was first designed as a microfluidic chip fabricated by simple laser ablation method. Fluids with melting point around the refrigerated temperature (2–8°C) were then screened. Peanut oil was identified to have a melting point around 6°C with fast response time and was used as the temperature responding fluid. Peanut oil was also mixed with coconut oil in a volume ratio of 5:1, 5:3, and 1:1 to obtain melting points at 12.5, 19, and 21°C, respectively. Next, a multiplex TTI was designed and was integrated with a resonant sensor to obtain a wireless, quantitative signal while responding at temperature thresholds of 9, 13.5, and 19.5°C. The resonant sensor coupled TTI showed a stepwise response as the temperature was incrementally increased above the temperature thresholds of the multiplex TTI. A transient temperature perturbation demonstrated that the TTI has an irreversible response with predictable time of temperature aberration. To demonstrate the utility of the resonant sensor coupled TTI in the ultra-cold chain application, a Styrofoam container containing dry ice was used as the model system. A TTI design containing 40% ethanol solution was used as the temperature responding fluid. As the dry ice within the container evaporated and the air temperature increased to above −35°C, the resonant frequency shifted by over a megahertz which serves as a clear signal for remediation action.

The TTI coupled resonant sensor exhibits potential in monitoring the integrity of agricultural and pharmaceutical products through global supply chains. Advantages include contact free measurement enabling positioning of the sensor within the package avoiding opportunities for tampering. It is also tunable to different temperature regimes based on the fluid used as the signal transduction agent. The facile fabrication would keep cost per unit low, allowing for multiple sensors to be placed throughout a large pallet allowing for assessment of any localized warm

zones. The multiplex feature enables the sensor to not only serve as an indication of product deterioration but also as a signal for preventative action. However, the designed sensor uses gravity as the driving force, requiring the sensor to be in the right orientation. Prior to use in a real scenario, accuracy and false positive rates must be assessed as well as scalable manufacturing processes. For monitoring over a longer period, the sensor response in the long term should be tested. A closed TTI design over an open atmospheric condition can increase the lifetime of the sensor.

CRediT authorship contribution statement

Nareen Anwar: Formal analysis, Investigation, Methodology, Validation. **Yee Jher Chan:** Conceptualization, Data curation, Formal analysis, Methodology, Supervision, Validation, Visualization, Writing – original draft, Writing – review & editing, Investigation. **Nigel Forest Reuel:** Funding acquisition, Project administration, Supervision, Writing – original draft, Writing – review & editing, Conceptualization.

Declaration of Competing Interest

The authors declare that they have no known competing financial interests or personal relationships that could have appeared to influence the work reported in this paper.

Data availability

Data will be made available on request.

Acknowledgment

This work was supported in part by NSF grant #1827578 and #EEC 1852125.

Appendix A. Supporting information

Supplementary data associated with this article can be found in the online version at doi:10.1016/j.sna.2024.115346.

References

[1] L. Ruiz-Garcia, L. Lunadei, Monitoring cold chain logistics by means of RFID, Sustain. Radio Freq. Identif. Solut. (2) (2010) 37–50.
[2] E. Derens-Bertheau, V. Osswald, O. Laguerre, G. Alvarez, Cold chain of chilled food in France, Int. J. Refrig. vol. 52 (2015) 161–167.
[3] A. Chaudhuri, I. Dukovska-Popovska, N. Subramanian, H.K. Chan, R. Bai, Decision-making in cold chain logistics using data analytics: a literature review, Int. J. Logist. Manag. vol. 29 (3) (2018) 839–861.
[4] J.W. Han, M. Zuo, W.Y. Zhu, J.H. Zuo, E.L. Lü, X.T. Yang, A comprehensive review of cold chain logistics for fresh agricultural products: Current status, challenges, and future trends, Trends Food Sci. Technol. vol. 109 (October 2020) (2021) 536–551.
[5] R. Badia-Melis, U. Mc Carthy, L. Ruiz-Garcia, J. Garcia-Hierro, J.I. Robla Villalba, New trends in cold chain monitoring applications - a review, Food Control vol. 86 (2018) 170–182.
[6] R. Manzini, et al., Sustainability and quality in the food supply chain. A case study of shipment of edible oils, Br. Food J. vol. 116 (12) (2014) 2069–2090.
[7] J.C.S. Dos Santos, et al., Optimized ultra-low power sensor-enabled RFID data logger for pharmaceutical cold chain, 2015 IEEE Bras. RFID (2016) 18–22.
[8] E. Abad, et al., RFID smart tag for traceability and cold chain monitoring of foods: demonstration in an intercontinental fresh fish logistic chain, J. Food Eng. vol. 93 (4) (2009) 394–399.
[9] H. Luo, M. Zhu, S. Ye, H. Hou, Y. Chen, L. Bulysheva, An intelligent tracking system based on internet of things for the cold chain, Internet Res vol. 26 (2) (2016) 435–445.
[10] R. Riem-Vis, Cold chain management using an ultra low power wireless sensor network, *WAMES 2004*, 2004.
[11] C.C. White, T. Cheong, In-transit perishable product inspection, Transp. Res. Part E Logist. Transp. Rev. vol. 48 (1) (2012) 310–330.
[12] F. Vivaldi *et al.*, A temperature-sensitive RFID tag for the identification of cold chain failures, *Sensors Actuators, A Phys.*, vol. 313, p. 112182, 2020.
[13] R. Bhattacharyya, C. Floerkemeier, S. Sarma, Low-cost, ubiquitous RFID-tag-antenna-based sensing, Proc. IEEE vol. 98 (9) (2010) 1593–1600.
[14] R. Bhattacharyya, C. Di Leo, C. Floerkemeier, S. Sarma, L. Anand, RFID tag antenna based temperature sensing using shape memory polymer actuation, Proc. IEEE Sens. (2010) 2363–2368.
[15] G.S. Lorite, et al., Novel, smart and RFID assisted critical temperature indicator for supply chain monitoring, J. Food Eng. vol. 193 (2017) 20–28.
[16] M. Martinez, D. Van Der Weide, Chipless RFID temperature threshold sensor and detection method, 2017 IEEE Int. Conf. RFID, RFID 2017 (2017) 61–66.
[17] H. El Matbouly, S. Tedjini, K. Zannas, Y. Duroc, Chipless RFID threshold temperature sensor compliant with UHF and ISM radio frequency, 2018 2nd URSI Atl. Radio Sci. Meet. -RASC 2018, (June) (2018) 3–6.
[18] E.M. Amin, N.C. Karmakar, B.W. Jensen, Fully printable chipless RFID multi-parameter sensor, Sens. Actuators, A Phys. vol. 248 (2016) 223–232.
[19] E.M. Amin, J.K. Saha, N.C. Karmakar, Smart sensing materials for low-cost chipless RFID sensor, IEEE Sens. J. vol. 14 (7) (2014) 2198–2207.
[20] S. Wang, X. Liu, M. Yang, Y. Zhang, K. Xiang, R. Tang, Review of time temperature indicators as quality monitors in food packaging, Packag. Technol. Sci. vol. 28 (10) (Oct. 2015) 839–867.
[21] L.T. Hao, et al., Tamper-proof time-temperature indicator for inspecting ultracold supply chain, ACS Omega vol. 6 (12) (2021) 8598–8604.
[22] P. Suppakul, D.Y. Kim, J.H. Yang, S.B. Lee, S.J. Lee, Practical design of a diffusion-type time-temperature indicator with intrinsic low temperature dependency, J. Food Eng. vol. 223 (2018) 22–31.
[23] L.G. Cencha, G.F. García, N. Budini, R. Urteaga, C.L.A. Berli, Time-temperature indicator based on the variation of the optical response of photonic crystals upon polymer infiltration, Sens. Actuators A Phys. vol. 341 (October 2021) (2022).
[24] Y. Galagan, W.F. Su, Fadable ink for time-temperature control of food freshness: Novel new time-temperature indicator, Food Res. Int. vol. 41 (6) (2008) 653–657.
[25] J.-R. Jhuang, S.-B. Lin, L.-C. Chen, S.-N. Lou, S.-H. Chen, H.-H. Chen, Development of immobilized laccase-based time temperature indicator by electrospinning zein fiber, Food Packag. Shelf Life vol. 23 (2020) 100436.
[26] D. Wu, et al., Development and characterization of an enzymatic time-temperature indicator (TTI) based on Aspergillus niger lipase, Lwt vol. 60 (2) (2015) 1100–1104.
[27] S. Yan, C. Huawei, Z. Limin, R. Fazheng, Z. Luda, Z. Hengtao, Development and characterization of a new amylase type time-temperature indicator, Food Control vol. 19 (3) (2008) 315–319.
[28] S. Choi, et al., A self-healing nanofiber-based self-responsive time-temperature indicator for securing a cold-supply chain, Adv. Mater. vol. 32 (11) (2020) 1–8.
[29] A.T. Jafry, H. Lim, W.K. Sung, J. Lee, Flexible time–temperature indicator: a versatile platform for laminated paper-based analytical devices, Microfluid. Nanofluidics vol. 21 (3) (2017) 1–13.
[30] S. Wang, X. Liu, M. Yang, Y. Zhang, K. Xiang, R. Tang, Review of time temperature indicators as quality monitors in food packaging, Packag. Technol. Sci. vol. 28 (10) (2015) 839–867.
[31] C. Zhang, et al., Time-temperature indicator for perishable products based on kinetically programmable Ag overgrowth on Au nanorods, ACS Nano vol. 7 (5) (2013) 4561–4568.
[32] J. Zeng, S. Roberts, Y. Xia, Nanocrystal-Based Time Temperature Indicators, Chem. Eur. vol. 16 (42) (2010) 12559–12563.
[33] S. Forghani, H. Almasi, M. Moradi, Electrospun nanofibers as food freshness and time-temperature indicators: A new approach in food intelligent packaging, Innov. Food Sci. Emerg. Technol. vol. 73 (April) (2021) 102804.
[34] Q.A. Huang, L. Dong, L.F. Wang, LC passive wireless sensors toward a wireless sensing platform: status, prospects, and challenges, J. Micro Syst. vol. 25 (5) (2016) 822–841.
[35] S. Charkhabi, K.J. Jackson, A.M. Beierle, A.R. Carr, E.M. Zellner, N.F. Reuel, Monitoring wound health through bandages with passive LC resonant sensors, ACS Sens. vol. 6 (1) (2021) 111–122.
[36] A.R. Carr, et al., Sweat monitoring beneath garments using passive, wireless resonant sensors interfaced with laser-ablated microfluidics, npj Digit. Med. vol. 3 (1) (2020).
[37] S. Charkhabi, et al., Effects of fabrication materials and methods on flexible resonant sensor signal quality, Extrem. Mech. Lett. vol. 41 (2020) 101027.

Yee Jher Chan is a PhD candidate in the Department of Chemical and Biological Engineering at Iowa State University. His research focuses on improving agricultural and biological processes through smart materials and tools development.

Nigel Forest Reuel is Associate Professor of Chemical and Biological Engineering at Iowa State University. His research focuses on contact-free sensors for closed systems such as biomanufacturing vessels, agricultural fields, and embedded wearables.